

THE IMPACT OF PEDOCLIMATE ON SOIL SUBGROUP DEVELOPMENT IN A SEMI-ARID REGION OF IRAN

Behzad MOHAMMADHOSSEINI SAGAYESH^{1*}, Ali Asghar JAFARZADEH¹,
Farzin SHAHBAZI¹ & Asghar FARAJNIA²

¹Soil Science Department, Faculty of Agriculture, University of Tabriz, Iran; ajafarzade@tabrizu.ac.ir;
shahbazi@tabrizu.ac.ir

²East Azerbaijan Agricultural and Natural Resources Research and Training Center, Tabriz, Iran;
farajnia1966@yahoo.com

*Corresponding author: behzadmohammadhosseini@gmail.com

Abstract: Understanding the relationship between climate and soil even on low levels of categories i.e., subgroups become increasingly vital. Pedoclimate was defined as a microclimate within the soil that can be identified by determining soil moisture and temperature regimes. This study focuses on evaluating soil subgroup development under different pedoclimate conditions across a semi-arid region of Iran. Based on the Java Newhall simulation model and climatic data from 52 meteorological stations over 30 years (1992-2022), the pedoclimate class was modeled. Using data from 670 soil profiles across the East Azerbaijan Province of Iran, the profile development index (PDI) was determined. Subsequently, the soils were classified into 12 subgroups. To create the final soil maps, a geopedological approach utilizing a weighted overlay technique was implemented, considering the influences of geology, topography, and land use. According to the Java Newhall simulation model, five distinct pedoclimatic zones were identified as follows: Mesic-Dry Xeric (46.58 %), followed by Thermic-Weak Aridic (23.97 %), Mesic-Typic Xeric (23.94 %), Thermic-Typic Aridic (5.37 %), and Frigid-Typic Xeric (0.14 %). The soil orders ranked by area extent are: Inceptisols (43.36 %) > Entisols (32.29 %) > Aridisols (21.31 %) > Mollisols (1.46 %). It was found that Entisols were under all pedoclimate classes while Inceptisols were identified only under the Xeric moisture regime. Based on the PDI values (on average), Typic Calcixerolls and Lithic Xerorthents respectively show the highest and the lowest development levels (29.6 and 6.7). Further visualization revealed that all Typic Calcixerolls were overlaid under the Mesic-Typic Xeric class. Moreover, there were no subgroups of Mollisols in the Aridic and Thermic classes. Interestingly, Xeric Haplocambids showed a similar development with Typic Haploxerepts. The study establishes the importance of pedoclimates in soil classification and development influenced by climate. Its findings enhance soil resource management and support new hypotheses and insights in various soil science fields.

Keywords: East Azerbaijan Province, Geopedology, Java Newhall, Soil Map, Weighted Overlay.

1. INTRODUCTION

Climate significantly influences soil formation by affecting precipitation, temperature, and evapotranspiration, which in turn impacts soil characteristics, genesis, development, evolution, and overall physical, chemical, and biological properties (Certini & Scalanghe, 2023). Pedoclimate is directly influenced by the climatic characteristics of the soil formation site, including the amount, intensity, and distribution of precipitation, daily and monthly temperature fluctuations, sunlight radiation, vegetation

cover and so forth (Freppaz et al., 2019). The term pedoclimate refers to the temporal patterns of soil moisture and temperature over a specified period, recognized in the context of soil moisture and temperature regimes (SMR and STR, respectively) (Bonfante et al., 2011). The SMR and STR refer to the amount of water retained and the temperature at a specific depth of soil for a defined era within a year (USDA, 2022). Since moisture and temperature are the primary factors driving various processes in soil, determining the SMR and STR plays a significant role in soil resource management. SMR and STR are

related to soil classification, land suitability, biological activity, and nutrient mobility (Vankova et al., 2021). The concept of pedoclimate involves determining SMR and STR through field studies, which are often time-consuming and expensive. The Java Newhall Simulation Model (JNSM) has been widely used for determining SMR and STR in recent years. It estimates both regimes based on the precipitation and temperature data, demonstrating high accuracy when using long-term (at least 20 years) climatic statistics (Costantini et al., 2002). Karaca & Sargin (2022) showed that when using JNSM, annual calendars detailing soil moisture and temperature conditions were produced in addition to the maps of pedoclimate classes. Consequently, it serves as an important practical tool for studies and management of soil and water resources across the area.

As mentioned in the above content, SMR and STR are among the most important factors in soil classification, as they are utilized in defining two of the 12 soil orders at the highest classification category in soil taxonomy, as well as in many suborders (Bockheim et al., 2014). At lower classification categories, such as family, the class of STR is one of the ten characteristics used in this category of classification system (Stolt et al., 2021). An examination of the various microclimates present in the region can provide valuable insights into the role of pedoclimate in the classification and development of soils (Gelybó et al., 2018).

As we know, integrating multiple soil-field properties formalizes equations in assessing soil development. According to ancient literature (Bilzi & Ciolkosz, 1977; Harden & Taylor, 1983), various soil morphological data have been widely used in pedogenic observations for decades, either as a profile or a horizon represented in a compact numerical value. In this regard, it has been found that the soil profile development index (PDI) is an important index for evaluating soil development when comparing soil profiles or horizons in terms of the degree of pedogenesis and also examining the effect of soil formation factors on soil development, such as soil climate conditions (Koop et al., 2020). Since soil development is significantly affected by different microclimates in vast areas with semi-arid conditions (Jafarian et al., 2023), it is expected that a reasonable relationship between soil development and pedoclimate will be found in the East Azerbaijan province of Iran.

One of the essential requirements for a better understanding of the role of soil formation factors and processes, as well as for comparing their impacts on the development of soils in a region with a complex landscape, is the preparation of a soil classification

map (Esfandiarpour Borujeni et al., 2009). Generally, soil mapping aims to divide the soil continuum into natural categories by employing mapping units that exhibit greater homogeneity for specific characteristics compared to the continuum in its entirety (Baruck et al., 2016). There are several methods for delineating soil map units, one of which is the geopedological approach (Zinck, 1989). A geopedological approach integrates geomorphology, the study of landform formation, with pedology, which focuses on soil formation, to explore the interconnections between landforms and soils while investigating how geological and geomorphic factors influence soil development, classification, and distribution (Samiei-Fard et al., 2024). Among these, the weighted overlay technique can facilitate the preparation of final classification maps by utilizing the principles of the geopedology approach and collecting foundational base maps (González-Arqueros et al., 2018).

Finally, this research aims to explore the role of pedoclimate on soil subgroup development in the East Azerbaijan province of Iran as a semi-arid region.

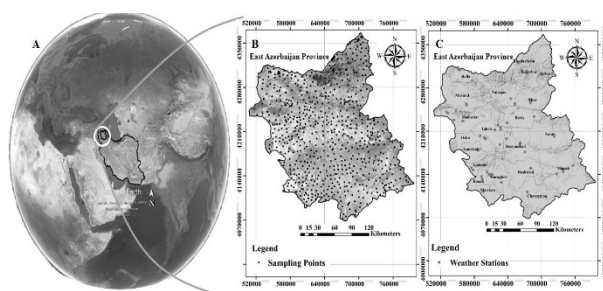


Figure 1. Location of East Azerbaijan Province in Iran (a), the described soil profiles across the study area (b), and meteorological station locations at counties of the study area (c).

2. MATERIALS AND METHODS

2.1. General description of the study area

The East Azerbaijan Province, covering an area of over 45756 km², is located in the northwest of Iran (Figure 1a). The geographical coordinates of this province range from 36°45' to 39°26' north latitude and from 45°05' to 48°22' east longitude, placing it within the UTM 38 zone of the Northern Hemisphere. The elevation above sea level in the province varies from 126 to 4163 meters. According to the Extended de Martonne climate classification system (Khalili et al., 2022), this province is categorized as semi-arid, with a mean annual total precipitation of 250 to 300 mm over the past three decades (from 1992 to 2022) and a mean annual temperature ranging from 8.9 to 15.8 °C across different areas (IRIMO, 2022). The

diverse topography of the province has led to the formation of various microclimates in different areas.

2.2. Climatic data collection

In this study, climatic data including the mean monthly total precipitation and the mean monthly temperature over 30 years (from 1992 to 2022) were extracted from records of 52 climatological and synoptic weather stations located in the study area. The geographical locations of these stations are illustrated in Figure 1c (IRIMO, 2022). The analysis of changes in climatic conditions during the study period was conducted through a time series examination of the mean annual total precipitation and mean annual temperature in the study area using the Mann-Kendall test (Kendall, 1975). The Mann-Kendall test is a non-parametric rank-based test used to determine the significance of linear and non-linear trends. In this test, the null hypothesis (H_0) and the alternative hypothesis (H_1) correspond to the absence of a trend contrasted with the presence of a trend, respectively, in the time series of observational data (Vivekanandan, 2024).

2.2.1. Pedoclimate modelling

To determine the SMR and STR in terms of pedoclimate classes in the study area, the JNSM was employed using climatic data (Waltman et al., 2011). This model is essentially an updated version of the older Newhall Simulation Model (NSM) developed by Franklin Newhall (Newhall, 1972). The processing algorithm of this model is based on the concepts defined in the Keys to Soil Taxonomy (USDA, 2022) (Table 1). The core of this model requires fundamental input information, including the mean monthly total precipitation and mean monthly temperature over 30 years, as well as ancillary data comprising the geographical coordinates (elevation, latitude, and longitude) of the study area. For execution and processing, after entering air temperature data, the model necessitates defining a coefficient to balance the mean monthly air temperature with soil temperature. Given the lack of comprehensive, extensive, and precise studies on certain soil characteristics, such as soil temperature with high accuracy for all stations across the study area over 30 years, the validation of existing soil temperature data was conducted using values derived from various empirical equations from previous studies (Barman et al., 2017; Zadmehr & Farrokhan Firouzi, 2020) to estimate soil temperature based on air temperature. According to the keys to soil taxonomy (USDA, 2022), the control section for soil temperature is defined at 50 cm above the soil surface.

Comparative analysis of results obtained from different empirical equations and available

measured data indicated that soil temperature in medium-textured soil at field capacity and in upper 50 cm of soil is approximately 1 °C higher than air temperature. To minimize estimation errors in various modeling scenarios, adjustments of 0.5 and 2 °C were used instead of 1 °C. Due to a significant increase in the mean annual temperature over the past three decades and a reduction in temperature discrepancies among stations in the province, the final results in the STR classes showed no significant differences compared to the coefficient of 1 °C, at least in the upper 50 cm of soil. Furthermore, according to the concepts outlined in Table 1, the model for executing and determining SMR requires only the input of mean monthly total precipitation and mean monthly temperature. The model's output is provided in XML file format, which includes classes and subclasses of SMR and STR, daily calendars of soil moisture and temperature, as well as a graph of precipitation-evapotranspiration potential predicted by the model (using the Thornthwaite method) for the study area.

The output of the JNSM for pedoclimate classes is based on results from weather stations that have point distributions. However, environmental studies typically require an examination of land areas. Therefore, point data must be extrapolated to cover broader regions. Given the qualitative nature of the model's output data, traditional methods such as geostatistical techniques cannot be employed to extend the model's results spatially. Consequently, it appears that utilizing climatic data from the nearest weather station to the study area is a viable solution to overcome this limitation. For this purpose, the Thiessen polygon method, which is one of the most common approaches for delineating study units based on proximity to a given location, was employed using ArcMap software (Thiessen, 1911). In this method, each selected weather station is enclosed within a polygon, and the entire area contained within that polygon is assigned a value equal to that of the corresponding point, which represents the qualitative output results from the JNSM for the reference station.

2.3. Soil profile data collection

In this study, in addition to the 520 available pre-existing soil data points, a total of 150 soil profiles were dug during June and July 2020 using a random sampling approach (Figure 1b). It is well understood that pre-existing soil data and maps play a crucial role in studies of soil science (Hendriks et al., 2019). Piikki et al. (2021) advised that a brief description of the sampling design uncovers site-

Table 1. Concepts of Newhall model processing algorithm (USDA, 2022).

SMR	subclasses	Summary of characteristics in soil moisture control section
Aridic		Generally hot and dry conditions
	Weak Aridic	Moist or partially moist > 45 but < 90 consecutive days when soil temperature is $> 8^{\circ}\text{C}$
	Typic Aridic	Moist or partially moist ≤ 45 consecutive days when soil temperature is $> 8^{\circ}\text{C}$
	Extreme Aridic	Completely dry during the whole year
Xeric		Generally moist in winter and dry in summer
	Typic Xeric	Dry in all parts for 45 to ≤ 90 consecutive days in summer
	Dry Xeric	Dry in all parts for > 90 consecutive days in summer
STR		Mean annual soil temperature at 50 cm depth
Cryic		Mean annual soil temperature is $0\text{--}8^{\circ}\text{C}$
Frigid		Mean annual soil temperature is similar to Cryic but with warmer summer soil temperatures
Mesic		Mean annual soil temperature is $8\text{--}15^{\circ}\text{C}$
Thermic		Mean annual soil temperature is $15\text{--}22^{\circ}\text{C}$

specific soil background, even if the samples were gathered in a previous survey. The information on the analyses of soil morphological characteristics (Singer, 2005) and physicochemical characteristics (Van Reeuwijk, 2002) was collected for the 520 pre-existing soil profiles. Additionally, these characteristics were described and determined for the 150 complementary soil profiles collected in the field. Finally, morphological and physicochemical data for 2893 soil horizons were compiled from a total of 670 studied soil profiles. Based on the results of these analyses, the soils of the study area were classified according to the soil taxonomy system, up to the subgroup category (USDA, 2022).

2.3.1. Quantifying soil development

Soil development is often qualitative, making precise comparisons difficult. Quantifying soil development addresses this limitation by integrating morphological and analytical laboratory data into a single index. This process normalizes soil-field properties for each horizon (Figure 2) in a given chronosequence (Harden, 1982). The literature shows that PDI was initially formalized by Bilzi & Ciolkosz (1977). Harden & Taylor (1983) included two new properties for carbonate-rich soils in addition to the previously defined eight properties for quantitative comparison of soil development in four climatic regimes in the United States. Since the aforementioned index has been used numerous times in pedogenic investigations for decades (Tsai et al., 2007), it was therefore implemented in this research. The PDI has primarily consisted of weight-averaged normalized scores of 10 various morphological data i.e., total texture (texture class plus type of stickiness and plasticity), structure (grade and shape), clay films (abundance, thickness, and location), melanization, color-lightening, rubification, color-paling, dry consistency, moist consistency, and acidity.

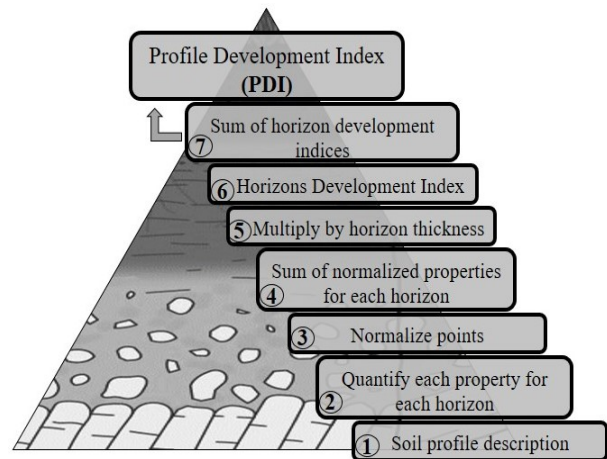


Figure 2. Steps for calculating the Profile Development Index (Harden & Taylor, 1983).

2.3.2. Preparation of soil classification map

Soil mapping serves as an essential tool in the physical environment for informed land planning and effective environmental management, striking a balance between economic and social development and the conservation of natural resources. The distribution of soils across the landscape is influenced by various soil-forming factors (da Silva et al., 2014). In this regard, the geopedological approach integrates an understanding of the geomorphic conditions under which soils evolve with field observations. Generally, the geopedological approach, initially developed by Zinck (1989), represents a systematic application of geomorphic analysis aimed at soilscape mapping. The geopedological approach has been used for separating more homogeneous land units and for increasing the purity of mapping units. In this approach, first, gathering preliminary data is crucial. This includes collecting geological, topographic, and land use maps. These datasets help in understanding the landscape's features, underlying rock types, and environmental conditions, providing a contextual backdrop for the soil mapping (Rossiter, 2023). To achieve this, the weighted overlay

technique was utilized in ArcGIS software, assigning a weight of one hundred percent to each input data set. Currently, various studies have utilized the weighted overlay technique for mapping different soil characteristics (Zeng et al., 2024). Specifically, the weights of geology, topography, and land use were assigned as 45 %, 45 %, and 10 %, respectively. The outcome of this operation is the production of an initial map of soil units. Subsequently, to create the final soil units map, the characteristics of the soil profiles in the study area were examined with respect to their corresponding units. Based on the established soil taxonomy level, homogeneous units are ultimately dissolved and delineated (Figure 3) (Zinck, 2023). In this study, two levels of soil taxonomy, namely orders and subgroups, were mapped.

3. RESULTS AND DISCUSSIONS

3.1. Climatic data analysis and pedoclimate classes

The overall statistical description of mean monthly temperature and mean monthly total precipitation in the study area, based on data extracted from 52 synoptic and climatological stations, is presented in Table 2 for the period from 1992 to 2022. According to the results in Table 2, the coldest and warmest months of the studied years were January and August, respectively, while April was identified as the wettest month and August as the driest month.

The results obtained from the Mann-Kendall test further corroborate the findings presented in Figure 4, demonstrating that during the examined era (1992 to 2022), the mean annual temperature significantly increased at the 5 % significance level ($Z = +3.18$), while the decrease in mean annual total precipitation was not statistically significant ($Z = -$

0.56) (Table 3). This overall trend in temperature and precipitation changes suggests the occurrence of climate change over time in the study area, which has also been reported in previous studies related to agriculture and soil resources within the study area (Pournaji et al., 2023; Niknam et al., 2018).

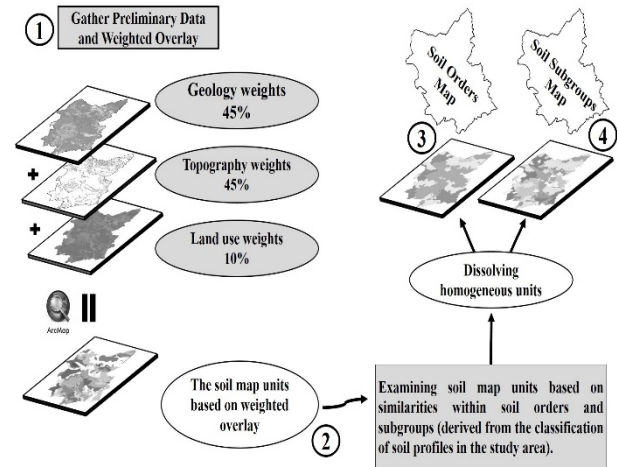


Figure 3. A comprehensive overview of the process for creating soil classification maps throughout the study area.

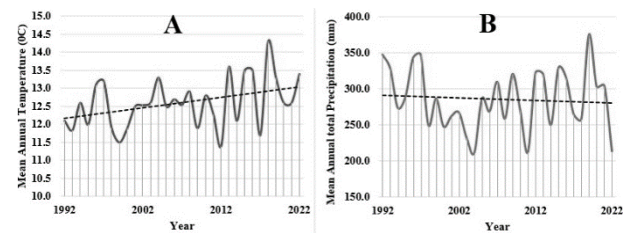


Figure 4. Mean annual temperature (a) and mean annual total precipitation (b) during 1992- 2022 in the study area (Num. of Stations: 52).

The output of the JNSM for all the studied stations is similar to the sample presented in Figure 5 for the Tabriz station, which is organized into three sections:

Table 2. Statistic description of mean monthly temperature and mean monthly total precipitation during 1992 - 2022 in the study area (Num. of Stations: 52).

Months	Precipitation (mm)					Temperature (°C)				
	Min	Max	Mean	SD	CV (%)	Min	Max	Mean	SD	CV (%)
January	12.0	28.4	20.4	4.21	21	-4.7	3.2	-0.8	1.8	-*
February	13.0	43.7	27.8	7.98	29	-2.5	3.0	0.5	2.0	-*
March	22.2	60.9	34.9	10.14	29	3.2	8.8	5.9	2.0	33
April	14.9	59.7	46.0	9.63	21	7.7	20.0	11.2	2.8	25
May	29.5	75.5	42.2	11.41	27	12.8	20.0	16.1	2.2	14
June	0.7	40.0	14.7	9.19	63	17.6	26.1	21.8	2.6	12
July	1.1	15.4	6.9	4.38	63	20.3	29.5	25.3	2.9	12
August	0.4	9.7	3.8	2.78	72	20.8	29.7	25.6	3.0	12
September	2.5	25.3	8.7	5.55	63	16.9	25.5	21.6	2.5	12
October	1.9	32.9	19.3	7.67	40	11.1	18.1	15.0	1.9	13
November	18.7	38.3	30.5	5.68	19	4.0	11.3	7.7	1.7	22
December	11.9	42.0	26.2	8.19	31	-1.6	4.9	2.0	1.5	77

Note:*In the months of January and February, due to the low mean temperature in °C, CV cannot be calculated

the precipitation-potential evapotranspiration graph (Figure 5a), daily soil temperature and moisture calendars (Figure 5b), and classes and subclasses of SMR and STR (Figure 5c).

Table 3. Mann-Kendall values for mean annual temperature and mean annual total precipitation trend during 1992 - 2022 in the study area.

	Mean annual temperature	Mean annual total precipitation
Z	+3.18	-0.56
Sig	**	-
Qmean	0.044	-0.56
Qmin99	0.009	-2.83
Qmax99	0.079	2.38
Qmin95	0.019	-2.007
Qmax95	0.074	1.75

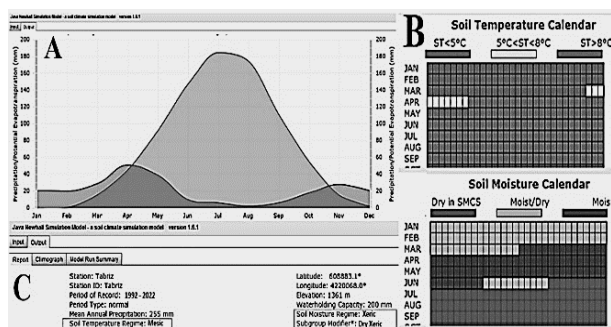


Figure 5. Example of JNSM Output (Tabriz metrological station).

The results related to the precipitation-potential evapotranspiration graph at the stations indicate that, in all examined regions, the rate of evapotranspiration exceeds that of precipitation from mid-April to mid-October over six months. The soil moisture and temperature calendars extracted from the model for the stations are based on the temperature and moisture levels defined in the model's algorithm, which classifies the days of the year according to climatic conditions regarding soil moisture and temperature into three levels. This alignment shows a trend of moisture changes corresponding with temperature changes in the direction of increasing temperature and decreasing moisture, and vice versa; however, changes in soil moisture occur with a slight time lag relative to temperature. Furthermore, these results not only serve as necessary preprocessing for determining SMR and STR but can also be utilized in establishing agricultural calendars and large-scale agricultural planning in conjunction with the results obtained from land suitability assessments as noted by Karaca & Sargin (2022) in their research. The outcome of the model used, which determines the SMR and STR in the study area, indicates that various regions exhibit aridic and xeric moisture regimes as well as mesic, thermic, and frigid temperature regimes.

To create a map of the pedoclimate in the study area, the first step involved delineating the areas monitored by the meteorological stations. In this context, based on the number and distribution of the meteorological stations, the Thiessen method was applied to define the areas under the influence of each station. Figure 6 presents the pedoclimate map of the study area, derived from the JNSM. This map indicates that the study area consists of five distinct pedoclimatic zones, with the largest and smallest zones corresponding to the Mesic-Dry Xeric and Frigid-Typic Xeric classes, respectively (Table 4).

Table 4. The area and relative percentage of the pedoclimate classes and subclasses in the study area.

SMR	Subclasses	Area (km ²)	Area (%)
Aridic	Weak Aridic	10966.95	23.97
	Typic Aridic	2457.62	5.37
	Dry Xeric	21314.12	46.58
Xeric	Typic Xeric	11017.31	24.08
STR	Subclasses	Area (km ²)	Area (%)
Thermic	-	13424.57	29.34
Mesic	-	32267.73	70.52
Frigid	-	63.7	0.14
Pedoclimate Classes		Area (km ²)	Area (%)
Mesic-Dry Xeric		21314.12	46.58
Thermic-Weak Aridic		10966.95	23.97
Mesic-Typic Xeric		10953.61	23.94
Thermic-Typic Aridic		2457.62	5.37
Frigid-Typic Xeric		63.7	0.14

Approximately half of the areas in the study area (46.58 %) consist of central and eastern regions characterized by the Dry Xeric SMR. Following this, the Weak Aridic SMR covers a significant portion of the western margin and part of the southeastern region (23.97 %), while the Typic Xeric regime primarily encompasses the highlands and northeastern area of the study area (24.08 %). In contrast, the Typic Aridic regime is present in a smaller area (5.37 %) in the northwest. An examination of the STR in the study area demonstrates that the western margins and parts of southeastern, which constitute 29.34 % of the study area, have a Thermic temperature regime. Additionally, the Frigid temperature regime is observed in a limited area of the eastern section, covering only 0.14 % of the study area. Meanwhile, the remaining parts of the study area are characterized by the Mesic STR. According to Sharma et al. (2010) and Rusu et al. (2017) management decisions, particularly at the regional level, are contingent upon a proper understanding of the relationships between climate and soil. Therefore, it can be asserted that soil

development and evolution, as well as their identification and Sustainable Agriculture management, are influenced by pedoclimate. Given recent climatic changes, it is essential to update maps of soil moisture and temperature regimes over different time eras.

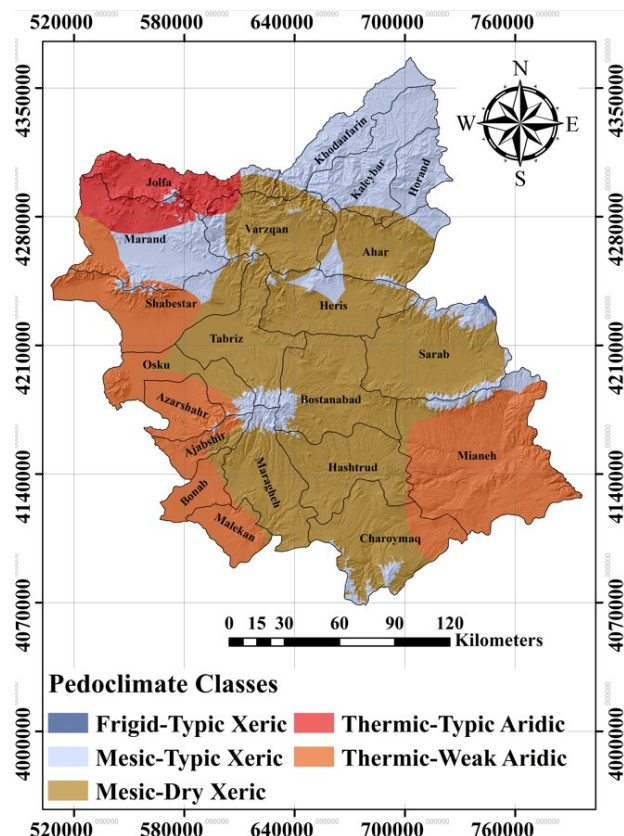


Figure 6. Pedoclimate classes zoning across the study area.

3.2. Distribution zoning maps of soil orders and subgroups

After the weighted overlay of the necessary preliminary data such as geology, topography, and land use in the geopedological approach, an initial distribution of map units is created. The soil profiles located within each of these map units are examined, and based on the classification of soils in the study area, homogeneous units are merged and dissolved. In this context, the highest and lowest levels of soil classification in this research, namely the orders and subgroups of soils, were examined. Consequently, the final maps of soil orders (Figure 7a) and subgroups (Figure 7b) are produced.

According to the Soil orders zoning map (Figure 7a), the largest area of soils in the study area is attributed to Inceptisols (43.36 %), followed by Entisols (32.29 %), Aridisols (21.31 %), and Mollisols (1.46 %).

Furthermore, Inceptisols have a greater number of subgroups compared to other soils in the study area (Figure 7b). Specifically, for Inceptisols, Aridisols, Entisols, and Mollisols, a total of 4, 3, 3, and 2 subgroups have been identified, respectively (Figure 8 and Table 5). While identical landform units may exhibit different soils at the family and series levels when determining soil subgroups. The remaining area extent (1.58 %) is classified as badlands and East Shore of Urmia Lake.

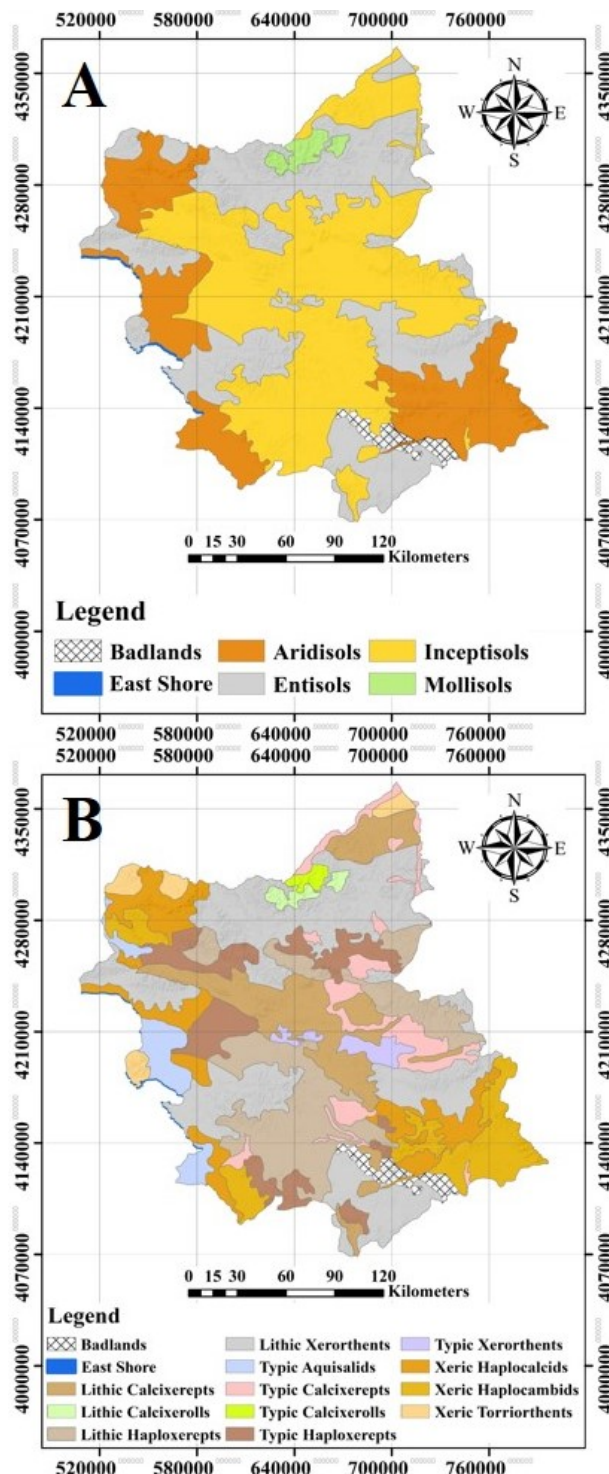


Figure 7. Soil orders (a) and subgroups (b) zoning map across the study area.

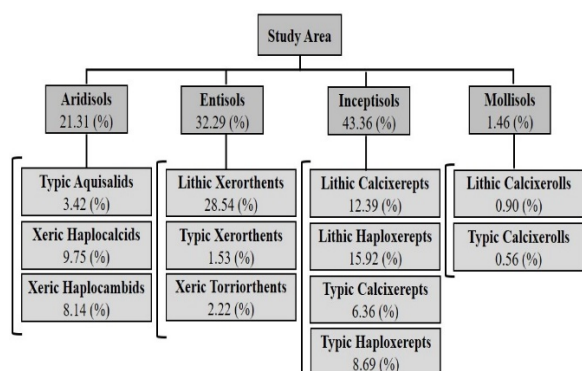


Figure 8. The area diagram of soil orders and subgroups extracted from zoning maps in the study area.

Table 5. The area occupied by each of the soil classification levels in the study area.

Soil Orders	Soil Subgroups	Area (km ²)
Aridisols	Typic Aquisalids	1563.87
	Xeric Haplocalcids	4461.59
	Xeric Haplocambids	3724.10
Entisols	Lithic Xerorthents	13058.33
	Typic Xerorthents	699.22
	Xeric Torriorthents	1016.63
Inceptisols	Lithic Calcixerepts	5668.44
	Lithic Haploxerepts	7286.23
	Typic Calcixerepts	2910.16
	Typic Haploxerepts	3976.98
Mollisols	Lithic Calcixerolls	410.13
	Typic Calcixerolls	256.93

3.3. Soil profile data analysis

Table 6 illustrates the descriptive statistics of PDI as raw data. The mean value and its CV were 14.91 and 38.58 % respectively. Overall, the studied index can be categorized as having moderate variability across the study area based on the classes defined by Fang et al. (2012).

Table 6. Statistical description of soils PDI (n = 670).

Statistical description	PDI
Min	2.55
1stQu	10.57
Median	15.51
Mean	14.91
3rdQu	18.92
Max	38.40
Skewness	0.19
Kurtosis	0.15
SD	5.75
CV (%)	38.58

Based on classification of soil up to the subgroup level according to the Keys to Soil Taxonomy (USDA, 2022), twelve soil subgroups were identified within four orders: Aridisols, Entisols, Inceptisols, and Mollisols in the study area.

Table 7 shows the variation of PDI associated with soil subgroups in the study area. The lowest amount of PDI was found for Entisols subgroups, as expected. Interestingly, Entisols were generally found on the top of mountains exhibiting very little or no profile development (Padmanabhan & Reich, 2023). The PDI normalized by area within soil order boundaries shows that the highest value was for Mollisols (on average 28.91), followed by Aridisols (on average 16.83), Inceptisols (on average 15.59) and Entisols (on average 7.08).

Table 7. The summary of the statistical description of soil subgroups PDI across the study area.

Soil Subgroups	PDI		
	Mean	SD	CV
Lithic Calcixerolls (LCL)	16.8 ^c	1.22	7.26
Lithic Calcixerepts (LCX)	13.7 ^d	2.15	15.69
Lithic Haploxerepts (LHX)	12.8 ^d	4.09	31.95
Lithic Xerorthents (LXO)	6.70 ^g	2.56	38.21
Typic Aquisalids (TAS)	12.1 ^{ed}	1.99	16.45
Typic Calcixerolls (TCL)	29.6 ^a	5.34	18.04
Typic Calcixerepts (TCX)	19.6 ^b	3.46	17.65
Typic Haploxerepts (THX)	16.4 ^c	3.87	23.60
Typic Xerorthents (TXO)	9.90 ^f	2.15	21.72
Xeric Haplocambids (XHB)	17.2 ^c	2.64	15.35
Xeric Haplocalcids (XHC)	18.2 ^{bc}	3.09	16.98
Xeric Torriorthents (XTO)	10.1 ^{fe}	2.89	28.61

Note: *Different letters indicate a significant difference in the comparison of means according to the Duncan test at a significance level of 5%.

The results strongly imply that the highest variation in the PDI values among developed/developing soil orders relative to Entisols was recorded for Mollisols with the highest significance difference (4.08-fold), followed by Aridisols (2.37-fold) and Inceptisols (2.20-fold) (Figure 9). This finding clearly shows that Inceptisols are quite young and starting to develop (Galbraith & Engel, 2005). Generally, our findings may be explained by the idea that various factors control the formation of the above-mentioned soil orders. For instance, climate not only plays a direct role in the development of Mollisols but also exerts an indirect influence by affecting vegetation (organisms as soil-forming factors), which serves, while, in Aridisols, climate alone has the most significant impact on soil development. Regardless of soil great groups, the normalized by area within their boundaries showed that the soils in lithic subgroups are weakly developed soils compared with the rest subgroups. One interpretation can be applied to the differences in development between the non-lithic subgroups of Inceptisols is that horizon development index values for calcic horizons were significantly greater than those of cambic horizons, similar to TCX (19.6^b on

average) and THX (16.4° on average). Disregarding lithic subgroups, among the subgroups related to Aridisols, the highest degree of development is associated with XHC (18.2^{bc} on average), followed by XHB (17.2° on average), and finally TAS (12.1^{ed} on average). The degree of development between XHC and XHB is relatively close, and significant differences in the factors contributing to their formation cannot be established; the parent materials may account for the observed discrepancies. However, regarding TAS, we obtained evidence that the east Shore of Urmia Lake indicates a transition area from unripe to ripened soils by Lake Bathymetry (Shahbazi et al., 2023).

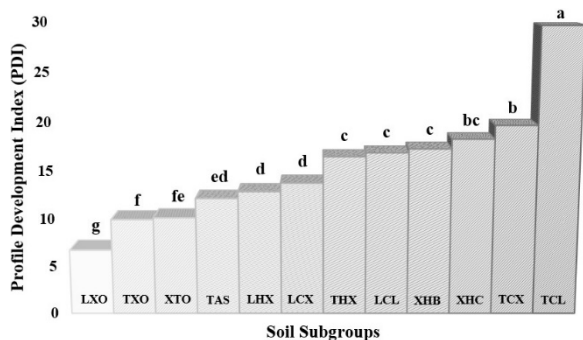


Figure 9. The chart compares the PDI means of different subgroups across the study area according to the Duncan test at a significance level of 5%.

3.4. Soil subgroup development in different pedoclimate classes

Table 8 illustrates the area of each soil subgroup under different pedoclimate classes across the study area. Pedoclimate is the primary factor used to determine two orders (i.e., the highest level of classification) in soil taxonomy, one of which is Aridisols. Regarding the Aridisols in the studied area, all TAS subgroups are under the Aridic SMR, with 98.49% classified as Weak Aridic subclass. For the remaining two subgroups of Aridisols, namely XHC and XHB, 97.37 % and 97.86 %, respectively, are also under the Aridic SMR. A small portion of these two subgroups that do not fall under the Aridic SMR corresponds to the Xeric moisture regime in the Dry Xeric subclass. Areas referred to as "Xeric border to Aridic" (between the Weak Aridic and Dry Xeric subclasses) represent transitional zones regarding moisture regimes, which can be temporarily influenced by short-term climatic changes, allowing for the transient presence of XHC and XHB subgroups. The results indicate that Entisols are present across all pedoclimates in the studied area (Ozsoy & Aksoy, 2011; USDA, 2022).

Specifically, Entisols are soils with little to no

development, characterized by properties determined by their parent materials (Grossman, 1983). None of the Inceptisol subgroups are found under the Aridic SMR according to the keys to soil taxonomy (USDA, 2022). Inceptisols with lithic contact, such as LCX and LHX, are entirely situated within the Xeric SMR, predominantly in the Dry Xeric subclass (more than 75 %). The lack of adequate moisture may contribute to the limited development of these Inceptisols. The remaining Inceptisol subgroups are distributed across two subclasses within the Xeric SMR. Mollisols constitute only a slight portion (1.46 %) of the northern to northeastern part of the studied area, with two subgroups identified. Mollisols, particularly the TCL subgroup, exhibited greater development compared to other soils examined in this study (Table 7 and Figure 9). The TCL subgroup is exclusively found in the Typic Xeric subclass of the Xeric SMR (100 %), while the lithic contact subgroup of Mollisols in the study area, namely LCL, is also present in the Dry Xeric subclass. Climatic conditions and consequently SMR have a direct and significant impact on soil development in semi-arid regions (Maren et al., 2015).

STR plays a direct role in the development and evolution of soils, as well as an indirect role by influencing SMR (Buol, 2013) (Table 1). The results show that the Thermic STR, covering 29.34 % of the studied area, is only associated with the Aridic SMR and has not been identified alongside the Xeric SMR. Thus, it can be inferred that within the Thermic STR, only Aridisols and Entisols are present. Also, the Frigid temperature regime, which encompasses a very small portion of the study area (part of the Sabalan mountain range located in the eastern part of the study area), includes Entisols with the LXO subgroup.

The findings of this study, along with their contribution to advancing research and the implementation of soil resource management practices, can play a crucial role in identifying areas susceptible to pollutant leaching and environmental consequences, as well as in addressing the challenges posed by climate change. By analyzing the obtained maps, it becomes possible to determine the types of soils in the region characterized by high permeability and suitable moisture levels, which increase the likelihood of groundwater contamination (Paltineanu et al., 2021, 2022). Furthermore, this information can be instrumental in water resource management and agricultural and environmental planning to reduce the use of fertilizers and chemical pesticides. Ultimately, a better understanding of thermal and moisture patterns can facilitate the development of more effective strategies for preserving the quality of soil and water resources and mitigating their pollution.

Table 8. The area of soil subgroups under pedoclimate classes across the study area.

Pedoclimate classes	Soil subgroups area (%)											
	LCL	LCX	LHX	LXO	TAS	TCL	TCX	THX	TXO	XHB	XHC	XTO
Frigid-Typic Xeric	0.00	0.00	0.00	0.12	0.00	0.00	0.00	0.00	0.00	0.00	0.00	0.00
Mesic-Typic Xeric	63.88	33.40	15.99	35.73	0.00	100.00	25.27	26.93	0.00	0.00	0.00	22.84
Mesic-Dry Xeric	36.12	66.60	84.01	37.52	0.00	0.00	74.73	73.07	100.00	2.14	2.62	0.00
Thermic-Weak Aridic	0.00	0.00	0.00	22.51	98.49	0.00	0.00	0.00	0.00	91.34	73.48	24.97
Thermic-Typic Aridic	0.00	0.00	0.00	4.12	1.51	0.00	0.00	0.00	0.00	6.52	23.89	52.20

4. CONCLUSION

An analysis of climatic parameters in the study area over 30 years (1992 - 2022) indicated a significant increase in temperature and a non-significant decrease in precipitation, suggesting gradual climate change. Modeling the pedoclimate revealed that the soils predominantly exhibit Xeric and Aridic SMR, as well as Mesic, Thermic, and Frigid STR. The northwestern regions have drier and warmer conditions. A geopedological approach using a weighted overlay technique for soil mapping units proved effective. The PDI was effective in assessing soil development and its relationship with pedoclimate. Analysis showed diverse levels of soil development, with climate being a key factor. Entisols were present in all pedoclimate classes, while Inceptisols were found only within the Xeric SMR. Typic Calcixerolls, with the highest development level, are entirely within the Mesic-Typic Xeric class, and no Mollisols were identified in Aridic and Thermic SMR and STR. Xeric Haplocambids and Xeric Haplocalcids from Aridisols showed similarities with Typic Haploxerepts and Typic Calcixerepts from Inceptisols. Subgroups with lithic contact demonstrated weaker development compared to others.

Overall, the role of pedoclimates in soil classification and development due to climatic influences has been established. The findings contribute to soil resource management and can aid in formulating new hypotheses in soil science.

Acknowledgments

The authors would like to thank the University of Tabriz for its support in conducting the PhD dissertation of the first author. This research did not receive any specific grant from funding agencies in the public, commercial, or not-for-profit sectors.

REFERENCES

- Barman, D., Kundu, D.K., Pal, S., Chakraborty, A.K., Jha, A.K., Mazumdar, S.P., Saha, R. & Bahattacharyya, P., 2017. *Soil temperature prediction from air temperature for alluvial soils in lower Indo-Gangetic plain*. International Agrophysics 31, 9-22, <https://doi.org/10.1515/intag-2016-0034>.
- Baruck, J., Nestroy, O., Sartori, G., Baize, D., Traidl, R., Vrščaj, B., Bräm, E., Gruber, F.E., Heinrich, K. & Geitner, C., 2016. *Soil classification and mapping in the Alps: The current state and future challenges*. Geoderma 264, 312-331, <https://doi.org/10.1016/j.geoderma.2015.08.005>.
- Bilzi, A.F. & Ciolkosz, E.J., 1977. *Time as a factor in the genesis of four soils developed in recent alluvium in Pennsylvania*. Soil Science Society of America Journal 41, 122-127, <https://doi.org/10.2136/sssaj1977.03615995004100010033x>.
- Bockheim, J.G., Gennadiyev, A.N., Hartemink, A.E. & Brevik, E.C., 2014. *Soil-forming factors and Soil Taxonomy*. Geoderma 226, 231-237, <https://doi.org/10.1016/j.geoderma.2014.02.016>.
- Bonfante, A., Basile, A., Manna, P. & Terribile, F., 2011. *Use of Physically Based Models to Evaluate USDA Soil Moisture Classes*. Soil Science Society of America Journal, 75, 181-191, <https://doi.org/10.2136/sssaj2009.0403>.
- Buol, S.W., 2013. *TROPICAL SOILS / Humid Tropical*. Reference Module in Earth Systems and Environmental Sciences, <https://doi.org/10.1016/B978-0-12-409548-9.05324-0>.
- Certini, G. & Scalenghe, R., 2023. *The crucial interactions between climate and soil*. Science of the Total Environment 856, 159-169, <https://doi.org/10.1016/j.scitotenv.2022.159169>.
- Costantini, A., Castelli, F., Raimondi, S. & Lorenzoni, P., 2002. *Assessing Soil Moisture Regimes with Traditional and New Methods*. Soil Science Society American Journal 66, 1889-1896, <https://doi.org/10.2136/sssaj2002.1889>.
- da Silva, A.F., Pereira, M.J., Carneiro, J.D., Zimback, C.R.L., Landim, P.M.B. & Soares, A., 2014. *A new approach to soil classification mapping based on the spatial distribution of soil properties*.

- Geoderma 219, 106-116, <https://doi.org/10.1016/j.geoderma.2013.12.011>.
- Esfandiarpour Borujeni, I., Salehi, M.H., Toomanian, N., Mohammadi, J. & Poch, R.M., 2009.** *The effect of survey density on the results of geopedological approach in soil mapping: a case study in the Borujen region, Central Iran.* Catena 79, 18-26, <https://doi.org/10.1016/j.catena.2009.05.003>.
- Fang, X., Xue, Z., Li, B. & An, S., 2012.** *Soil organic carbon distribution in relation to land use and its storage in a small watershed of the Loess Plateau, China.* Catena, 88, 6-13, <https://doi.org/10.1016/j.catena.2011.07.012>.
- Freppaz, M., Viglietti, D., Balestrini, R., Lonati, M. & Colombo, N., 2019.** *Climatic and pedoclimatic factors driving C and N dynamics in soil and surface water in the alpine tundra (NW-Italian Alps).* Nature Conservation, 34, 67-90, <https://doi.org/10.3897/natureconservation.34.30737>.
- Galbraith, J.M. & Engel, R.J., 2005.** *Inceptisols*, in: *Lal, R (Ed), Encyclopedia of Soil Science - Two-Volume Set., 2nd edition.* CRC Press.
- Gelybó, G., Tóth, E., Farkas, C., Horel, A., Kása, I. & Bakacsi, Z., 2018.** *Potential impacts of climate change on soil properties.* Agrokémia és Talajtan Journal 67, 121-141, <https://doi.org/10.1556/0088.2018.67.1.9>.
- González-Arqueros, M.L., Mendoza, M.E., Bocco, G. & Castillo, B.S., 2018.** *Flood susceptibility in rural settlements in remote zones: The case of a mountainous basin in the Sierra-Costa region of Michoacán, Mexico.* Journal of Environmental Management, 223, 685-693, <https://doi.org/10.1016/j.jenvman.2018.06.075>.
- Grossman, R.B., 1983.** *Developments in Soil Science.* Elsevier 11, 55-90, [https://doi.org/10.1016/S0166-2481\(08\)70613-5](https://doi.org/10.1016/S0166-2481(08)70613-5).
- Harden, J.W., 1982.** *A quantitative index of soil development from field description: examples from a chronosequence in central California.* Geoderma 28, 1-28, [https://doi.org/10.1016/0016-7061\(82\)90037-4](https://doi.org/10.1016/0016-7061(82)90037-4).
- Harden, J.W. & Taylor, E.M., 1983.** *A quantitative comparison of soil development in four climatic regimes.* Quaternary Research, 20, 342-359, [https://doi.org/10.1016/0033-5894\(83\)90017-0](https://doi.org/10.1016/0033-5894(83)90017-0).
- Hendriks, C.M.J., Stoorvogel, J.J., Lutz, F. & Claessens, L., 2019.** *When can legacy soil data be used, and when should new data be collected instead?* Geoderma, 348, 181-188, <https://doi.org/10.1016/j.geoderma.2019.04.026>.
- IRIMO., 2022.** *Country climate analysis.* In: Islamic Republic of Iran Meteorological Organization, East Azerbaijan province center. Data sheet.
- Jafarian, N., Mirzaei, J., Omidipour, R. & Kooch, Y., 2023.** *Effects of micro-climatic conditions on soil properties along a climate gradient in oak forests, west of Iran: Emphasizing phosphatase and urease enzyme activity.* Catena, 224, <https://doi.org/10.1016/j.catena.2023.106960>.
- Karaca, S. & Sargin, B., 2022.** *Determination of Soil Moisture and Temperature Regimes with the Newhall Simulation Model: Example of Van Province.* Agricultural Sciences 32, 394- 413, <https://doi.org/10.29133/yyutbd.1053917>.
- Kendall, M.G., 1975.** *Rank Correlation Methods*; Griffin: London, UK.
- Khalili, A., Bazrafshan, J. & Cheraghalizadeh, M., 2022.** *A Comparative study on climate maps of Iran in extended de Martonne classification and application of the method for world climate zoning.* Journal of Agricultural Meteorology, 10, 3-16.
- Koop, A.N., Hirmas, D.R., Sullivan, P.L. & Mohammed, A.K., 2020.** *A generalizable index of soil development.* Geoderma, 360, e113898, <https://doi.org/10.1016/j.geoderma.2019.113898>.
- Maren, I.E., Karki, S., Prajapati, C., Yadav, R.K. & Shrestha, B.B., 2015.** *Facing north or south: Does slope aspect impact forest stand characteristics and soil properties in a semiarid trans-Himalayan valley?* Journal of Arid Environments, 121, 112- 123, <http://dx.doi.org/10.1016/j.jaridenv.2015.06.004>.
- Newhall, F., 1972.** *Calculation of soil moisture regimes from climatic record.* Rev. 4 Mimeographed, USDA-SCS, Washington, DC.
- Niknam, P., Shahbazi, F., Oustan, S. & Sokouti, R., 2018.** *Using microleis dss to assess the impact of climate change on land capability in the miandoab plain, Iran.* Carpathian Journal of Earth and Environmental Sciences, 13, 225-234, <https://doi.org/10.26471/cjees/2018/013/020>.
- Ozsoy, G. & Aksoy, E., 2011.** *Genesis and classification of Entisols in Mediterranean climate in Northwest of Turkey.* Journal of Food, Agriculture & Environment 9, 998- 1004.
- Padmanabhan, E. & Reich, P.F., 2023.** *World soil map based on soil taxonomy*, in: *Goss, M.J., Oliver, M. (Eds), Encyclopedia of Soils in the Environment (Second Edition), vol 4.* Academic Press, Elsevier, pp: 218-231, <https://doi.org/10.1016/B978-0-12-822974-3.00118-X>.
- Paltineanu, C., Domnariu, H., Marica, D., Lăcătușu, A.R., Popa, G.A., Grafu, I.A., & Neagoe, A.D., 2021.** *Fertilizers` leaching from the root system zone – a potential environmental risk for groundwater pollution in coarse and medium-textured soils.* Carpathian Journal of Earth and Environmental Sciences, 16, 139-150, <https://doi.org/10.26471/cjees/2021/016/162>.
- Paltineanu, C., Dumitru, S.I. & Lăcătușu A.R., 2022.** *Assessing land susceptibility for possible groundwater pollution due to leaching – a case study on Romania.* Carpathian Journal of Earth and Environmental Sciences, 17, 49-57, <https://doi.org/10.26471/cjees/2022/017/199>.
- Piikki, K., Wetterlind, J., Söderström, M. & Stenberg, B., 2021.** *Perspectives on validation in digital soil mapping of continuous attributes—a review.* Soil

- Use and Management, 37, 7-21, <https://doi.org/10.1111/sum.12694>.
- Pournaji, S., Rezaei, H. & Jafarzadeh, A.A., 2023.** *Climate suitability changes trend of East Azerbaijan province lands for strategic crops of Wheat and Barley in last decades.* Agricultural meteorology 11, 4-15, <https://doi.org/10.22125/agmj.2023.381559.1144>.
- Rossiter, D.G., 2023.** *Knowledge Is Power: Where Digital Soil Mapping Needs Geopedology.* In: Zinck, J.A., Metternicht, G., del Valle, H.F., Angelini, M. (eds) *Geopedology*. Springer, Cham. https://doi.org/10.1007/978-3-031-20667-2_9.
- Rusu, T., Coste, C.L., Moraru, P.L., Szajdak, L.W., Pop, A.L. & Duda, B.M., 2017.** *Impact of climate change on agro-climatic indicators and agricultural lands in the Transylvanian plain between 2008-2014.* Carpathian Journal of Earth and Environmental Sciences, 12, 23-34.
- Samiei-Fard, R., Heidari, A., Drohan, P. J., Mahmoodi, S. & Ghatrehsamani, S., 2024.** *The Effect of Using a Geopedological Approach in Determining Land Quality Indicators, Land Degradation, and Development (Case Study: Caspian Sea Coast).* Environments 11, 1-20, <https://doi.org/10.3390/environments11010020>.
- Shahbazi, F., Weber, T.K.D., Oustan, S., Alvyar, Z., Jeon, S. & Minasny, B., 2023.** *Uncovering the effects of Urmia Lake desiccation on soil chemical ripening using advanced mapping techniques.* Catena, 232, e107440, <https://doi.org/10.1016/j.catena.2023.107440>.
- Sharma, A., Bharat R., Rao K. K.V., Vittal, P.R., Ramakrishna, Y.S. & Amarasinghe, U., 2010.** *Estimating the potential of rainfed agriculture in India: Prospects for water productivity improvements.* Agricultural Water Management, 97, 23-30, <https://doi.org/10.1016/j.agwat.2009.08.002>.
- Singer, M.J., 2005.** *Pedology: basic principles*, in: Hillel, D. (Ed), *Encyclopedia of Soils in the Environment*. Elsevier 151-156, <https://doi.org/10.1016/B0-12-348530-4/00001-1>.
- Stolt, M.H., O'Geen, A.T., Beaudette, D.E., Drohan, P.J., Galbraith, J.M., Lindbo, D.L., Monger, H.C., Needelman, B.A., Ransom, M.D., Rabenhorst, M.C. & Shaw, J. N., 2021.** *Changing the hierarchical placement of soil moisture regimes in Soil Taxonomy.* Soil Science Society of America Journal 85, 488-500, <https://doi.org/10.1002/saj2.20219>.
- Thiessen, A.H., 1911.** *Precipitation averages for large areas.* Monthly weather review 39, 1082-1089.
- Tsai, H., Huang, W.S. & Hseu, Z.Y., 2007.** *Pedogenic correlation of lateritic river terraces in central Taiwan.* Geomorphology 88, 201-213, <https://doi.org/10.1016/j.geomorph.2006.11.004>.
- USDA., 2022.** *Keys to Soil Taxonomy, Thirteenth edition.* Soil Survey Staff, USA.
- Van Reeuwijk, L.P., 2002.** *Procedures for Soil Analysis, sixth edition.* International Soil Reference and Information Centre, FAO, 119p.
- Vankova, Z., Vitkova, M., Trakal, L., Seyedsadr, S., Miller, O.A., Vincent, K., Addo, N. & Komarek, M., 2021.** *Soil moisture influences performance of selected stabilizing amendments in soil remediation.* Geoderma, 402, <https://doi.org/10.1016/j.geoderma.2021.115307>.
- Vivekanandan, N., 2024.** *Trend analysis of rainfall data using Mann-Kendall test and sen's slope estimator.* I-manager's Journal on Civil Engineering 14, 18-24, <https://doi.org/10.26634/jce.14.2.21074>.
- Waltman, SW., Miller, D.A., Bills, B. & Waltman, W.J., 2011.** *JAVA Newhall simulation model – Update to a traditional soil climate simulation model.* Presented at the Fundamental for Life: Soil, Crop and Environmental Sciences. Soil Science Society of America annual meetings; San Antonio, TX, USA.
- Zadmehr, H. & Farrokhi Firouzi, A., 2020.** *Estimating Soil Temperature from Meteorological Data Using Extreme Learning Machine, Artificial Neural Network and Multiple Linear Regression Models.* Soil and Water research 51 4, 895-906.
- Zeng, Y., Shi, T., Liu, Q., Yang, C., Zhang, Z. & Wang, R., 2024.** *A geographically weighted neural network model for digital soil mapping of heavy metal copper in coastal cities.* Journal of Hazardous Materials 480, <https://doi.org/10.1016/j.jhazmat.2024.136285>.
- Zinck, J.A., 1989.** *Physiography and soils. Lecture Notes for Soil Students.* Soil Science Division. Soil Survey Courses Subject Matter: K6 ITC, Enschede, the Netherlands.
- Zinck, J.A., 2023.** *The Geopedologic Approach.* In: Zinck, J.A., Metternicht, G., del Valle, H.F., Angelini, M. (eds) *Geopedology*. Springer, Cham. https://doi.org/10.1007/978-3-031-20667-2_4.

Received: 19.03.2025

Revised: 03.04.2025

Accepted: 09.04.2025

Published: 11.04.2025